Available online at www.sciencedirect.com
ScienceDirect
Journal of Power Sources 168 (2007) 299–306
JOURNAL OF POWER SOURCES
www.elsevier.com/locate/jpowsour

Polyol-synthesized PtRu/C and PtRu black for direct methanol fuel cells

Junsong Guo [a], Gongquan Sun [a,*], Shiguo Sun [a], Shiyou Yan [a], Weiqian Yang [a], Jing Qi [a], Yushan Yan [b], Qin Xin [a]

[a] *Direct Methanol Fuel Cell Laboratory, Dalian Institute of Chemical Physics, Chinese Academy of Sciences, Dalian 116023, China*
[b] *Department of Chemical and Environment Engineering, University of California, Riverside, CA 92521, USA*

Received 30 January 2007; received in revised form 27 February 2007; accepted 28 February 2007
Available online 12 March 2007

Abstract

PtRu/C and PtRu black catalysts with nominal Pt:Ru atomic ratio of 1:1 are prepared by a modified polyol process (co-reduction of metal precursor salts) as anode catalysts for direct methanol fuel cells (DMFCs). Without the carbon support, PtRu nanoparticles tend to agglomerate, while the PtRu nanoparticles in PtRu/C have a good dispersion as shown by TEM. Both PtRu black and PtRu/C have the almost same alloy degree indicated by XRD, but PtRu supported on carbon could improve the influence of Ru on Pt toward methanol oxidization as shown by cyclic voltammetry. The microstructure of PtRu/C is further studied by high-resolution transmission electron microscopy (HRTEM), and the results indicate that the lattice constant of Pt in PtRu electrocatalyst has contracted despite a few parts of Pt not alloyed with Ru due to the lattice constant of Pt without contracting, which is further proved by the results of temperature-programmed reduction (TPR). Such parts of unalloyed Ru are further proved to have ability to reduce the methanol oxidation potential on Pt by comparing the catalytic behaviors of Pt/C and Pt + Ru/C prepared by mixing carbon with separately prepared Pt and Ru colloids. Moreover, the catalytic behaviors of PtRu black and PtRu/C are also compared with those of commercial ones.

Keywords: Direct methanol fuel cell; PtRu/C; PtRu black; Unalloyed Ru

1. Introduction

PtRu/C catalysts are the most effective anode catalysts of direct methanol fuel cells (DMFCs) due to the complete oxidation of methanol to CO_2 via a bifunctional mechanism, which involves the abstraction reaction of hydrogen through the adsorption of methanol on Pt, forming a CO-like intermediate species, and the complete oxidation of CO species to CO_2 promoted by OH group formed on neighboring Ru under relatively low potential [1–3]. It is desirable to reduce the thickness of catalyst layer to improve mass transportation, and thus PtRu/C with high metal loading or even unsupported PtRu black have been used in DMFCs [4]. However, the synthesis of highly dispersed supported and unsupported PtRu with uniform nanoparticle size remains challenges, especially for unsupported and supported electrocatalysts with high metal loading.

Recently, the polyol process is widely used to prepare Pt-based supported electrocatalysts. For example, Chen et al. and Liu et al. have reported a microwave method to prepare carbon black or carbon nanotubes supported Pt and PtRu catalysts [5,6]. We previously used a conductive heating method and synthesized Vulcan XC-72 supported Pt, PtSn, PtPd and PtRu electrocatalysts [7–10]. Bock et al. further studied the synthesis mechanism of Vulcan XC-72 supported PtRu electrocatalysts and found that glycolates produced from the oxidization of ethylene glycol stabilize the PtRu colloids [11]. From those reported results, highly dispersed Pt-based supported electrocatalysts with metal loading less than 60 wt.% can be obtained. However, there are still no reports on the synthesis of unsupported PtRu black by polyol process for DMFCs, and the effect of carbon support on catalytic activity is still unclear.

In this work, PtRu black and 30–15 wt.% PtRu/C with nominal Pt:Ru atomic ratio of 1:1 are prepared by a polyol process for DMFCs and their microstructures, oxidation states and activities are characterized and compared with commercial PtRu black and PtRu/C by X-ray diffraction (XRD), transmission electron

* Corresponding author. Tel.: +86 411 84379063; fax: +86 411 84379063.
E-mail address: gqsun@dicp.ac.cn (G. Sun).

0378-7753/$ – see front matter © 2007 Elsevier B.V. All rights reserved.
doi:10.1016/j.jpowsour.2007.02.085

microscopy (TEM), temperature-programmed reduction (TPR), single cell performance test, anode polarization voltammetry and methanol stripping voltammetry. The effects of carbon support, alloying degree and unalloyed Ru on catalytic behaviors are discussed.

2. Experiment section

2.1. Catalyst preparation

$H_2PtCl_6{\cdot}6H_2O$ and $RuCl_3$ were used as precursors for the PtRu catalysts. Vulcan XC-72 carbon black (Cabot Corp. $S_{BET} = 236.8\ m^2\ g^{-1}$) oxidized by concentrated H_2O_2 was used as catalyst support. 30–15 wt.% PtRu/XC-72 catalysts were prepared via the following procedure. Calculated $H_2PtCl_6{\cdot}6H_2O$ and $RuCl_3$ were added to the ethylene glycol solution to form a brown solution with 2 $mg_{Pt+Ru}\ mL^{-1}$ solvent. Then the pH value of the solution was increased to above 13 with solution of sodium hydroxide in ethylene glycol (EG). The solution was heated to 170 °C at a rate of 10 °C min^{-1} and kept at this temperature for 3 h to obtain brown-black sol. At this time, a calculated amount of XC-72 was added to the above sol and stirred for half an hour for the supported catalysts. For PtRu black catalysts, no carbon was added. When the above solution was cooled to 80 °C, an amount of diluted hydrochloric acid was added to adjust the pH value to below 3 in order to reduce the concentration of glycolate which acts as a stabilizer for the PtRu colloid. After the solution was stirred for 12 h to settle the PtRu nanoparticles at 80 °C, the obtained black product was filtered, washed and dried. The process of preparing 30–15 wt.% Pt + Ru/XC-72 is similar to the above process except that Pt and Ru colloids are separately prepared and mixed.

2.2. Membrane electrode assemblies and cells

The membrane electrode assemblies (MEAs) were fabricated according to the method in literature [12]. PtRu black, PtRu black (JM), 30–15 wt.% PtRu/XC-72, 30–15 wt.% Pt + Ru/XC-72, 30–15 wt.% PtRu/XC-72 (JM) (JM-samples purchased from Johnson Matthey Corp.) and 40 wt.% Pt/XC-72 (JM) were used as anode catalysts. Except for PtRu black and PtRu black (JM) with Pt loading of 2.66 mg cm^{-2}, the Pt loading of other anode catalysts is 1.33 mg cm^{-2}. 40 wt.% Pt/XC-72 (JM) served as cathode catalyst with the Pt loading of 1.4 mg cm^{-2}. The MEA was sandwiched between two stainless steel flow field plates to form a single cell with an active cross-sectional area of 4 cm^2.

2.3. Physical chemical characterization

XRD patterns were recorded with a Rigaku Rotalflex (RU-200B) X-ray diffractometer using Cu Kα radiation with a Ni filter. The tube current was 100 mA with a tube voltage of 40 kV. The 2θ angular region between 20° and 85° was explored at a scan rate of 5° min^{-1}. The morphology and microstructure of catalysts were investigated by using Tecnai F30 field emission high-resolution transmission electron microscope (HRTEM) (FEI Company) or JEOL JEM-2000EX for TEM and HRTEM images. TPR experiments were carried out on ChemBET 3000 (QuantaChrome Co.). The as-prepared catalysts were placed in a U-shape tube and were heated at 10 °C min^{-1} from 25 to 120 °C and held for 0.5 h and then cooled to room temperature under Ar. TPR experiments were performed under 10 vol.% H_2/Ar from 25 to 850 °C at 10 °C min^{-1}.

2.4. Electrochemical characterization

Electrochemical activities of catalysts were first measured by cyclic voltammetry (CV) using a standard three-electrode cell at the EG&G model 273 potentiostat/galvanostat station. The working electrode was a vitreous carbon disk electrode covered by a thin layer of Nafion-impregnated catalyst. A platinum gauze served as the counter electrode and a saturated calomel electrodes (SCE) was used as the reference electrode. CV test was conducted in a solution of 0.5 M H_2SO_4 + 1 M CH_3OH at room temperature. Later the electrochemical activities of catalysts in electrodes were further characterized by anode polarization voltammetry and methanol striping voltammetry. All above electrochemical experiments were carried at 75 °C with anode sides fed by 1 M methanol at a flow rate of 1 mL min^{-1}, and the cathode fed with humidified hydrogen at 0.1 MPa served as both reference and counter electrode, designated as a dynamic hydrogen electrode (DHE). The single cell performance was measured on a fuel cell test system (Arbin Instrument Corp.).

2.4.1. Anode polarization voltammetry

The anode potential was scanned at 1 mV s^{-1} starting at 0 V (versus DHE) and ending when the current reached 0.8 A.

2.4.2. Methanol striping voltammetry

The anode potential was held at constant potential of 0.1 V versus DHE for 40 min. During the first 20 min, methanol was adsorbed onto the anode fed with 1 M methanol at a flow rate of 1 mL min^{-1}. While during the second 20 min, the anode was washed with deionized water at a flow rate of 4 mL min^{-1} to remove un-adsorbed methanol. Later, the anode potential was cycled between 0.1 and 0.7 V at 20 mV s^{-1} for five cycles, and the first and fifth cycles were recorded.

3. Results and discussion

After adding some diluted HCl solution to drop the pH value to below 3, the stability of the PtRu colloid is destroyed by decreasing the concentration of the colloid stabilizer—glycolate. Consequently, the PtRu particles could deposit from the suspended phase, and PtRu/C and PtRu black catalysts could be prepared. Fig. 1 shows the morphologies of polyol-synthesized PtRu/C and PtRu black catalysts. It is observed that PtRu/C has better metal particle dispersion, while unsupported PtRu black tends to agglomerate. The structures of PtRu/C and PtRu black along with commercial catalysts are further characterized by XRD as shown in Fig. 2. The relative data calculated from XRD diffraction patterns by Scherrer formula are listed in Table 1. Except for a diffraction peak around 26.1° in the diffraction of carbon supported Pt or PtRu catalysts, which could be attributed

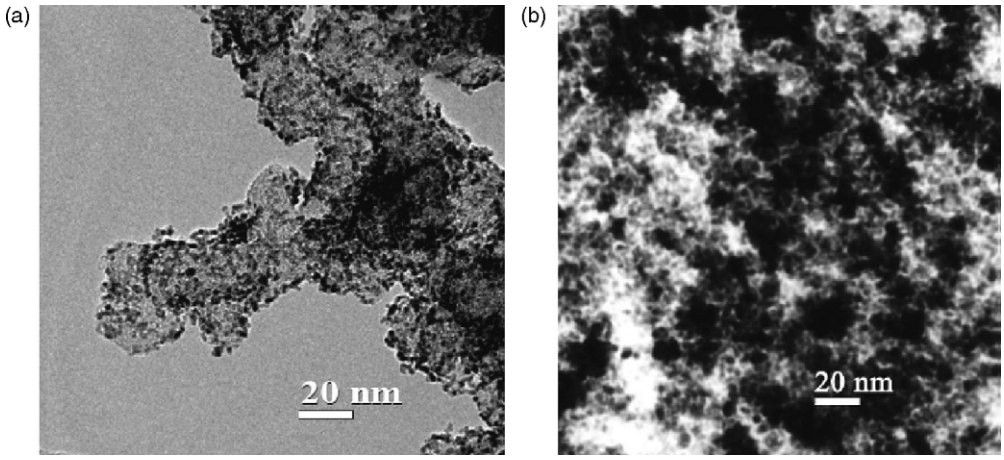

Fig. 1. TEM images of 30–15 wt.% PtRu/XC-72 (a) and PtRu black (b).

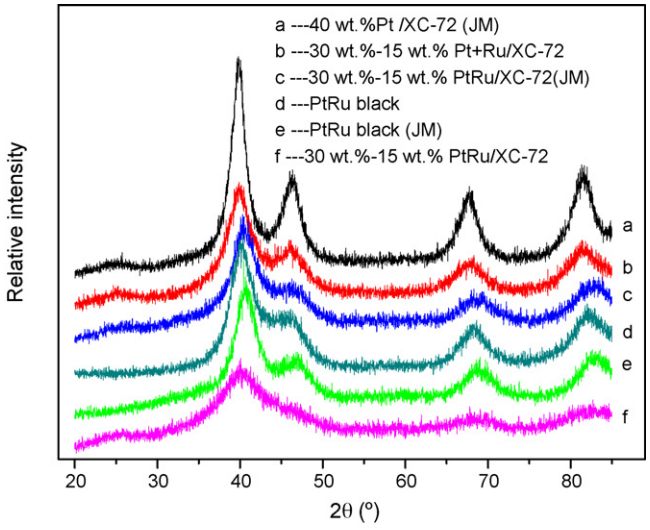

Fig. 2. XRD patterns of various catalysts.

to (0 0 2) crystalline plane of carbon with hexagonal structure, all the XRD patterns display the reflection characteristic of platinum face-centered cubic (fcc) crystal structure. Compared with the XRD pattern of 40 wt.% Pt/XC-72 (JM), the 2θ angle shifts of the Pt peaks reveal alloy formation between Pt and Ru. The lattice parameter of 30–15 wt.% PtRu/XC-72 and PtRu black is 0.3876 and 0.3879 nm, respectively, and in both cases, is smaller than that of 40 wt.% Pt/XC-72 (JM) (0.3914 nm, which is close to the reported 0.3916 nm). The results suggest that a part of Ru has entered into the crystal lattice of Pt. Calculated by the following formula [13]: $l_{PtRu} = 0.3916 - 0.124x_{Ru}$ (where l_{PtRu} is the lattice parameter of PtRu catalysts, and x_{Ru} is the percent of Ru in the PtRu alloy), the alloying degree is about 32.3 and 29.8%, respectively, for PtRu/C and PtRu catalysts, which shows co-reduction of Pt and Ru precursors can form alloyed PtRu catalysts, and carbon support hardly has any effects on alloying degree of PtRu catalysts prepared by polyol reduction method. In addition, compared with that of commercial 30–15 wt.% PtRu/XC-72 (JM) and PtRu black (JM), the alloying degrees of the polyol-synthesized PtRu/C and PtRu black catalyst are low, and there are about 70 or 50 wt.% of Ru residing in an amorphous phase for polyol-synthesized or commercial catalysts, respectively. So 30–15 wt.% Pt + Ru/XC-72 is prepared by mixing Pt and Ru colloids with carbon to study the effect of unalloyed Ru on methanol oxidation characteristics of Pt, and the XRD pattern is also shown in Fig. 2. The results show the lattice parameter of Pt shrinks very little from 0.3914 to 0.3910 nm, and the diffraction peaks of Ru hexagonal close-packing structures are not observed. Then 20 wt.% Ru/XC-72 was prepared by ethylene glycol reduction method, and the XRD pattern of 20 wt.% Ru/XC-72 is compared with that of Vulcan XC-72 as shown in Fig. 3. The diffraction peaks are very similar, which is probably due to the poor crystallization of polyol-synthesized Ru.

The microstructures of 40 wt.% Pt/XC-72 (JM), 30–15 wt.% PtRu/XC-72, and 20 wt.% Ru/XC-72 are further studied by HRTEM as shown in Fig. 4. For 40 wt.% Pt/XC-72 (JM), the 0.228 and 0.198 nm spacings with a slight positive equipment error in Fig. 4a are assigned to the Pt (1 1 1) and (2 0 0) planes (PCPDF#040802), respectively. While for 30–15 wt.%

Table 1
Data calculated from XRD patterns by Scherrer formula

Samples	Particle size (nm)	Lattice parameter (nm)	Pt (2 2 0) position (°)	Alloyed Ru (%)
30–15 wt.% PtRu/XC-72	1.82	0.3876	68.40	32.3
30–15 wt.% PtRu/XC-72 (JM)	2.20	0.3860	68.72	45.2
PtRu black	2.64	0.3879	68.34	29.8
PtRu black (JM)	2.45	0.3851	68.91	52.4
30–15 wt.% Pt + Ru/XC-72	2.40	0.3910	67.73	–
40 wt.% Pt/XC-72 (JM)	3.31	0.3914	67.64	–

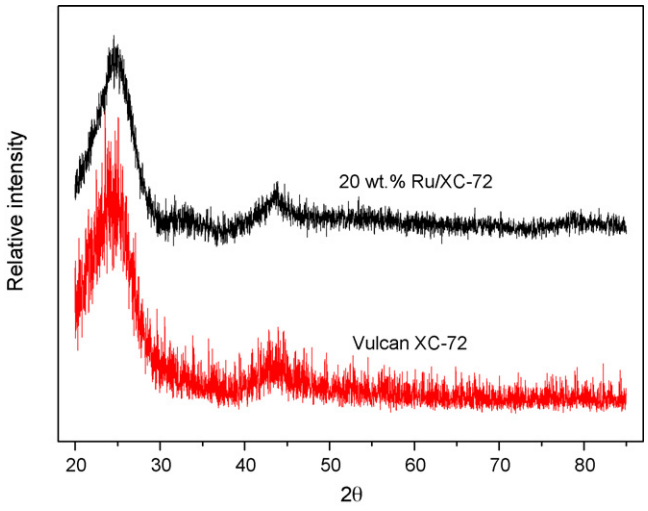

Fig. 3. XRD patterns of 20 wt.% Ru/XC-72 and Vulcan XC-72.

PtRu/XC-72, the 0.222, 0.223 and 0.224 nm spacings in Fig. 4b assigned to Pt (111) plane shrink distinctly compared with 0.228 nm of 40 wt.% Pt/XC-72 (JM), which shows that some of Ru have alloyed with Pt in co-reduction process. However, some platinum particles unalloyed with Ru do exist as shown by the un-contracted 0.228 and 0.227 nm spacings attributed to Pt (1 1 1) plane (Fig. 4b). This is probably due to the fact that some Ru^{3+} ions fail to be reduced simultaneously with Pt^{4+} ions as the redox potential of Ru^{3+}/Ru ($E_0 \sim 0.62$V) is much lower than that of Pt^{4+}/Pt ($E_0 \sim 0.74$V) [14]. The structures of Ru as indicated by XRD patterns (Fig. 3) are mostly in poor crystal form as shown in Fig. 4c.

To clarify the chemical states of Pt and Ru in polyol-synthesized PtRu catalysts, TPR experiments are carried out and the TPR profiles are shown in Fig. 5. The peaks at around 310 and 510 °C are assigned to the reduction of RuO_x to Ru, and of PtO_y to Pt, respectively. The carboxylic oxides on the surface of Vulcan XC-72 begin to be reduced at about 420 °C. The negative peaks forming between 80 and 320 °C could be attributed to the desorption of hydrogen adsorbed on the surface of Pt. Compared with the hydrogen desorption areas (HDA) of commercial PtRu black (2 5 5) and PtRu/C (3 6 2), these of polyol-synthesized PtRu black (4 7 4) and PtRu/C (6 0 5) are relative large, but these hydrogen desorption areas are still much lower than that of 40 wt.% Pt/XC-72 (JM) (1 4 6 6). This result indicates that when Pt and Ru form alloy, the concentration of H atoms around RuO_x locating on the surface of PtRu will be higher than that around RuO_x isolated from Pt. Then the reduction of RuO_x on the surface of PtRu alloy will become easy, and the onset reduction temperature of RuO_x will reduce. When the alloying degree decreases, the gap between Pt and Ru increases, and the role of adsorbed hydrogen on Pt for reducing the onset reduction temperature of RuO_x becomes weak. Thus, the desorption area of the catalyst could characterize the amount of Pt unalloyed with Ru. Small one represents high alloying degree, while large one represents low alloying degree. Moreover, when Pt and Ru form alloy, there is only one reduction peak between 310 and 510 °C for commercial PtRu black and PtRu/C. However, in the TPR profiles of polyol-synthesized PtRu black and PtRu/C, peaks around 310 and 510 °C still exist, which indicates some parts of Ru and Pt have not alloyed. This result is consistent with the result of HRTEM. From the TPR profiles of 20 wt.% Ru/XC-72 and 45 wt.% Pt + Ru/XC-72, polyol-synthesized Ru is in oxidized state, which is usually amorphous, and this result can explain why the structure of Ru appeares amorphous by

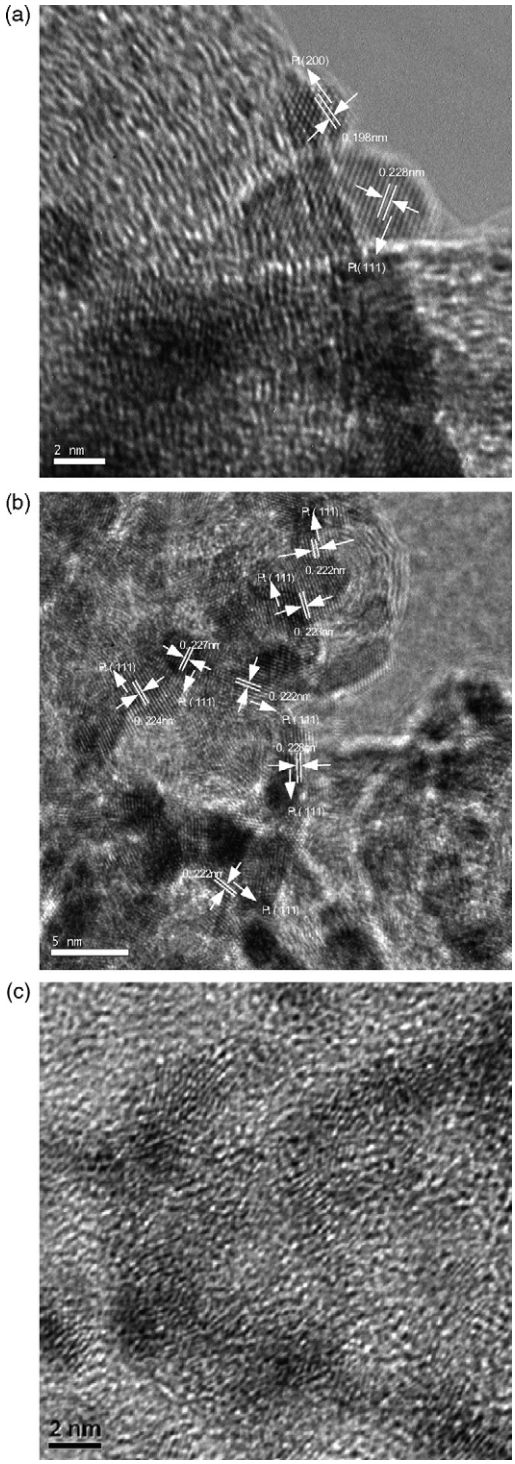

Fig. 4. HRTEM images of 40 wt.% Pt/XC-72 (JM) (a), 30–15 wt.% PtRu/XC-72 (b), and 20 wt.% Ru/XC-72 (c).

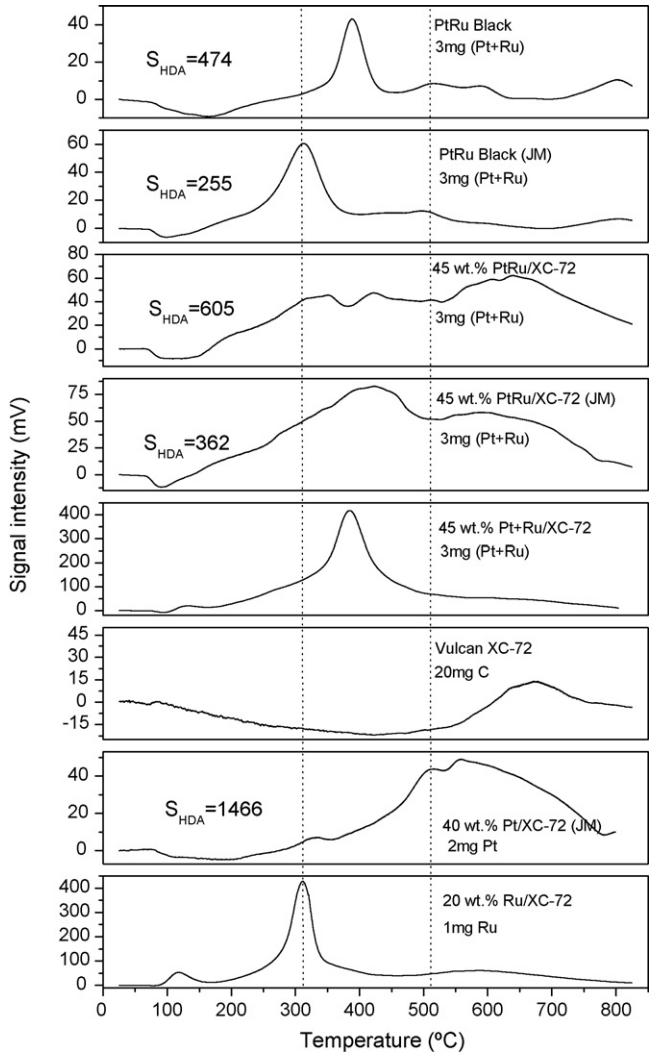

Fig. 5. TPR profiles of different samples under flowing gas of 10 vol.% H_2/Ar. Heating rate: 10 °C min^{-1}.

XRD. When polyol-synthesized PtRu catalyst by co-reduction of metal salts, the peak of Ru reduction decrease dramatically, which indicates Ru is in metal state when Ru entering the lattice of Pt, while unalloyed Ru and alloyed Ru exposing on the surface are in form of oxidized state.

The electrochemical activities toward methanol oxidation of the catalysts are characterized by CV in a solution of 1.0 M CH_3OH + 0.5 M H_2SO_4 at room temperature, and the fifth circles are recorded as shown in Fig. 6. The current density is normalized according to the amount of platinum to study the influence of Ru. Comparing the CV curves of 40 wt.% Pt/XC-72 (JM) and 30–15 wt.% PtRu/XC-72 (JM), the adding of Ru greatly reduces the onset methanol oxidation potential on Pt and methanol oxidation peak and peak position potential of backward potential sweeping. According to literatures [15,16], the formation of backward peak in CV is due to methanol oxidation on reactivated oxidized Pt sites. Therefore, adding Ru could reduce reduction potential of oxidized Pt and the amount of reactivated oxidized Pt sites in the potential range of backward peak formation, which means that it becomes difficult for reduction of oxidized Pt after adding Ru. Compared with 40 wt.% Pt/XC-72 (JM) under potential less than 0.454 V versus SCE, although the methanol oxidation potential of 30–15 wt.% Pt + Ru/XC-72 is distinctly observed to shift negatively, which further testifies that unalloyed Ru could reduce the methanol oxidation potential on Pt [17,18], the backward peak is greatly larger and shifts more anodically than that of 30–15 wt.% PtRu/XC-72 prepared by co-reduction of metal precursors, which indicates that a large amount of Pt in Pt + Ru/C still shows the catalytic characteristics of pure Pt, and the utilization of Ru is low. With the increase in alloying degree, the onset methanol oxidation potential of 30–15 wt.% PtRu/XC-72 further shifts to lower potential, and the backward methanol oxidation peak decreases, which shows that more amount of Pt are influenced by Ru and the utilization of Ru could be improved by co-reduction of Pt and Ru precursors. As for unsupported catalysts, although the forward methanol oxidation peak is larger than that of commercial PtRu black, and they have almost same onset methanol oxidation potential, the backward methanol oxidation peak is larger than that of commercial one. This is probably due to the low alloying degree of Pt in the polyol-synthesized PtRu black, and most of Ru residing where electrons could not arrive. Moreover, although alloying degrees of PtRu black and 30–15 wt.% PtRu/XC-72 are almost identical as shown by XRD, the backward methanol oxidation peak of PtRu/C is smaller than that of PtRu black, suggesting that the influence of Ru on Pt toward

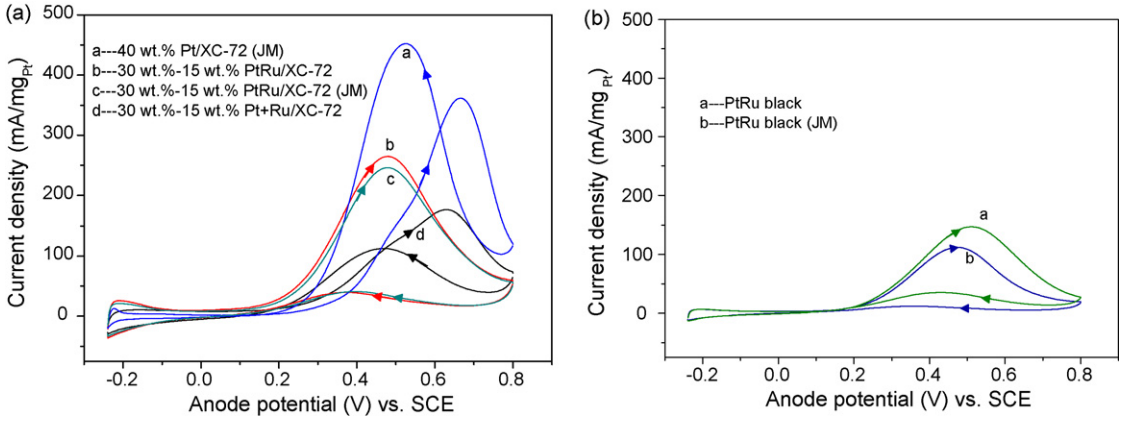

Fig. 6. Cyclic voltammetries of PtRu/C (a) and PtRu black (b) in 0.5 M H_2SO_4 + 1 M CH_3OH at 25 °C. Scan rate: 20 mV s^{-1}.

methanol oxidation could improve after PtRu nanoparticles supported on carbon. This may be due to that carbon support could provide electron conduits for more unalloyed Ru, and thus more Ru particles could provide OH species for alloyed or unalloyed Pt nanoparticles to oxidize methanol under lower potential. Moreover, although the alloying degree of polyol-synthesized PtRu/C is lower than that of commercial PtRu/C as shown by the results of XRD and TPR, the activity of polyol-synthesized PtRu/C is slightly higher than that of commercial one as shown in Fig. 6a.

Therefore, the above results indicate that the active material of Ru is unalloyed Ru, which is constituted by amorphous RuO_x. The activity of PtRu is not determined whether Pt and Ru form alloy or not, and it is determined by the dispersing degree of Pt and RuO_x, and the utilization of RuO_x. When Pt and Ru form alloy, although the dispersing degree of Pt and RuO_x could be improved, the utilization of Ru is likely low due to that alloyed Ru in body phase do not participate in the methanol oxidation reaction. From above discussion, the utilization of unalloyed Ru could be improved by co-reduction of Pt and Ru precursors or by supporting PtRu nanoparticles on carbon in polyol-synthesizing process.

Fig. 7 shows the anode polarization curves of the DMFCs with various catalysts. It is observed that methanol oxidation potential on 30–15 wt.% PtRu/XC-72 is the lowest among all the catalysts tested. More specifically, it shifts cathodically over 20 mV with respect to that of the second lowest methanol oxidation potential from 30–15 wt.% PtRu/XC-72 (JM) under same polarization current. The unalloyed 30–15 wt.% Pt + Ru/XC-72 has the highest methanol oxidation potential. However, compared with the anode polarization curve of 40 wt.% Pt/XC-72 (JM), the onset methanol oxidation potential on 30–15 wt.% Pt + Ru/XC-72 is lower by about 200 mV. This indicates unalloyed Ru could greatly reduce the methanol oxidation potential on Pt. Comparing anode polarization curves of the DMFCs with polyol-synthesized and commercial PtRu black, the curve of

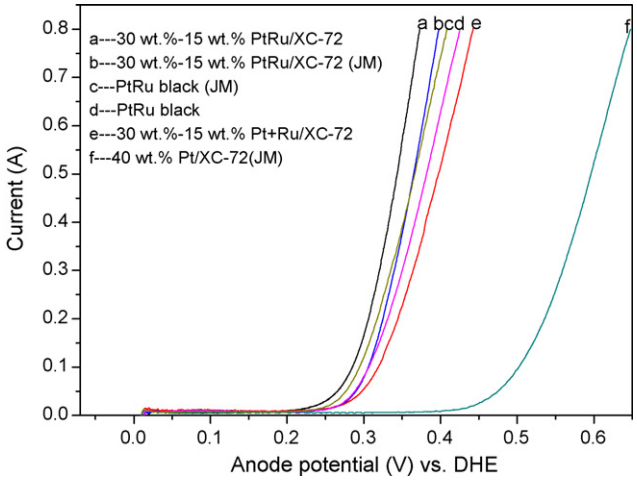

Fig. 7. Anode polarization curves of single cells with various catalysts. Cell temperature: 75 °C; scan rate: 1 mV s^{-1}; anode: 1 mol L^{-1} CH_3OH at a flow rate of 1.0 mL min^{-1}; cathode: humidified hydrogen under pressure of 0.1 MPa at a flow rate of 60 sccm.

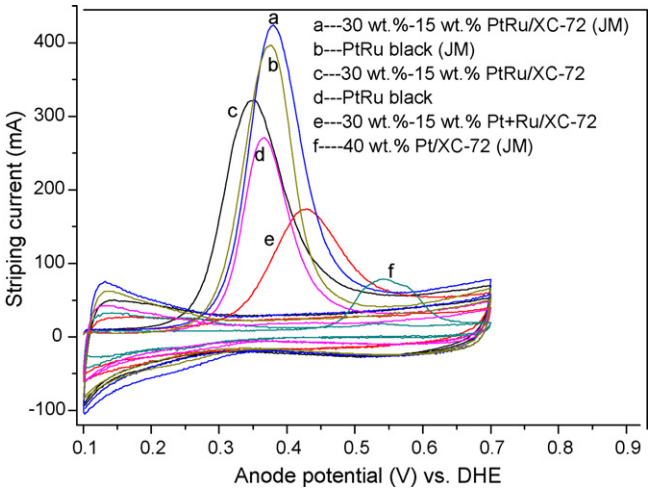

Fig. 8. Methanol stripping curves of anodes with various catalysts. Cell temperature: 75 °C; scan rate: 20 mV s^{-1}; anode: 1 mol L^{-1} CH_3OH at a flow rate of 1.0 mL min^{-1}; cathode: humidified hydrogen at pressure of 0.1 MPa with a flow rate of 60 sccm.

homemade PtRu black distinctly shifts to high potential by about 16 mV, which is likely due to that the utilization of unalloyed Ru is low and that a large amount of Pt in polyol-synthesized PtRu black shows pure Pt catalytic characteristics as indicated by the results of CV.

The comparison of the in situ stripping behavior of adsorbed methanolic residues for these catalysts is shown in Fig. 8. It is evident that with the addition of Ru by co-reduction of metal salts or by mixing metal colloids, the peak positions of PtRu catalysts shift toward lower potentials on account of the decrease in the activation energy for methanol removal with respect to 40 wt.% Pt/XC-72 (JM). By comparing the behaviors of PtRu black and 30–15 wt.% PtRu/XC-72, it is observed the 30–15 wt.% PtRu/XC-72 sample has the larger stripping area and lower potential of methanol oxidation. Such evidences indicate PtRu nanoparticles supported on carbon and prepared by co-reduction of metal salts have a larger amount of catalytic sites and relatively high activity. In addition, comparing polyol-synthesized PtRu/C and PtRu black with commercial PtRu/C and PtRu black, the methanol stripping areas of polyol-synthesized both PtRu/C and PtRu black catalysts are relative smaller and broader than those of commercial catalysts, but the methanol stripping peak positions of homemade catalysts shift to low anode potential by about 29 or 10 mV for PtRu/C and PtRu black, respectively. Such evidences indicate that large amount of unalloyed Pt make polyol-synthesized PtRu catalysts have a low stripping area, and unalloyed Ru could further decrease the methanol oxidation potential on alloyed Pt particles besides unalloyed ones.

The cell polarization and power density curves of the DMFCs with various catalysts at 75 and 90 °C are shown in Fig. 9. The results show that the DMFC with 30–15 wt.% PtRu/XC-72 as anode catalyst has the highest cell voltage under same discharging current density, and the highest discharge current density. Its maximum power density could achieve 159 and 205 mW cm^{-2} at 75 and 90 °C, respectively, which are significantly higher than

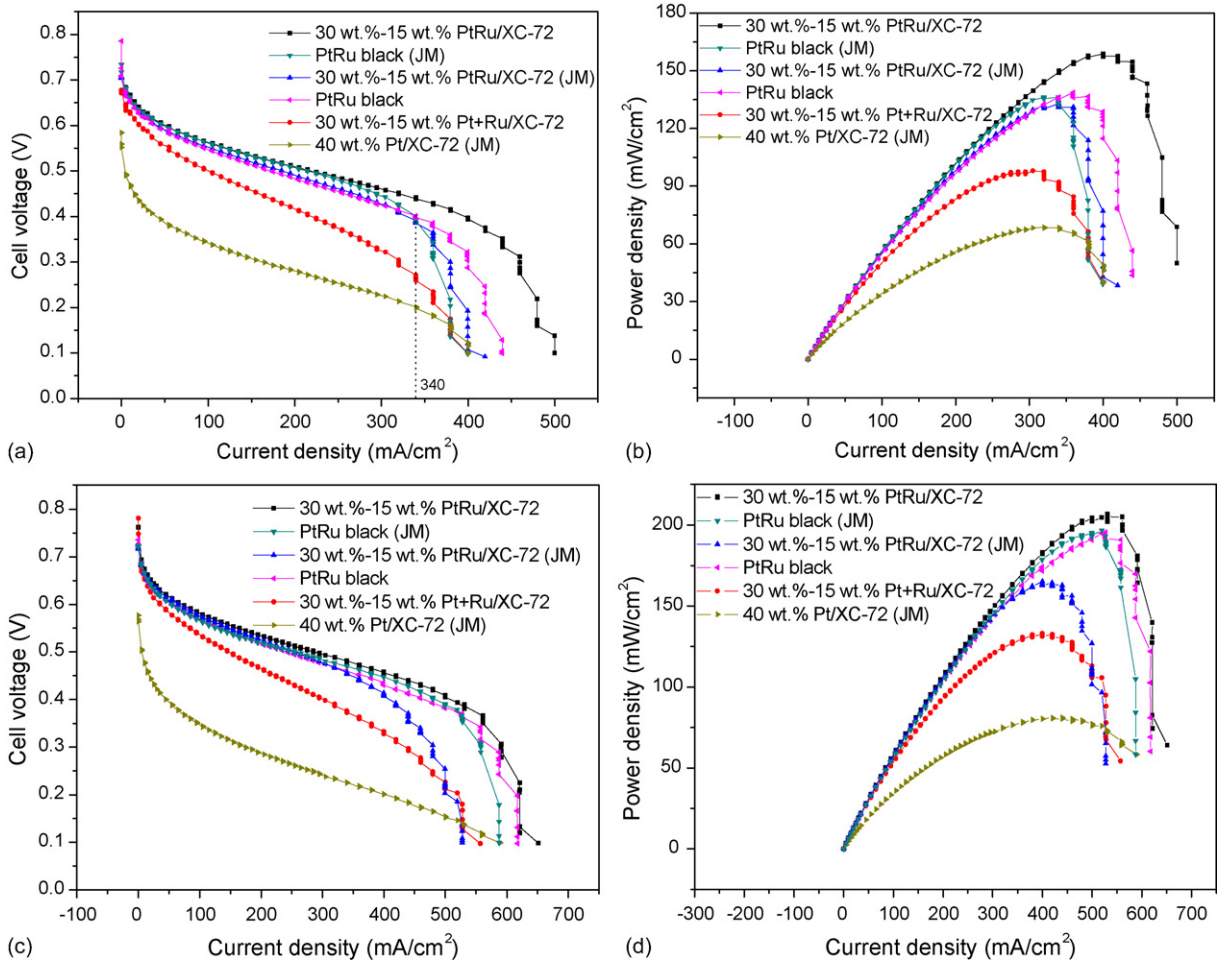

Fig. 9. Cell polarization (a and c) and power density (b and d) curves of DMFCs with various catalysts at 75 °C (a and b) and 90 °C (c and d). Methanol concentration: 1.0 mol L^{-1}; anode: 1 mol L^{-1} CH_3OH at a flow rate of 1.0 mL min^{-1}; cathode: non-humidified oxygen at pressure of 0.2 MPa with a flow rate of 200 sccm.

these achieved by using the commercial 30–15 wt.% PtRu/XC-72 (JM) catalyst (136 and 165 mW cm^{-2}). Comparing the performances of the DMFCs with polyol-synthesized and commercial PtRu black at 75 °C, the cell voltage of the DMFC with polyol-synthesized PtRu black is lower than that of commercial one under the current density of 340 mA cm^{-2} as shown in Fig. 9a, but the highest achievable discharge current is higher for the DMFC with polyol-synthesized PtRu black. With cell temperature increased to 90 °C, the gaps of cell voltage of the DMFCs with polyol-synthesized and commercial PtRu black decrease. These results indicate that lower utilization of unalloyed Ru and more Pt showing catalytic characteristics of pure Pt in the polyol-synthesized PtRu black cause the DMFC to produce low voltage, but the active sites could increase by improving the anode potential and cell working temperature. Moreover, comparing the performances of the DMFCs with PtRu black and PtRu/C as shown in Fig. 9b and d, the effect of working temperature on PtRu black catalyst is more significant than on PtRu/C, which is probably due to better mass transport property in the PtRu black catalyst layer with thin thickness. The performance of the DMFC with 30–15 wt.% Pt + Ru/XC-72 is the poorest when compared with other PtRu catalysts prepared by co-reduction, but it is much higher than that with 40 wt.% Pt/XC-72 (JM), which means that unalloyed Ru reduces methanol oxidation potential on Pt.

4. Conclusion

In summary, PtRu black and PtRu/C have been prepared by ethylene glycol reduction method for DMFCs, and the effects of carbon support, alloying degree and unalloyed Ru on catalysts' activities have been investigated. Without the carbon support, PtRu black tends to agglomerate, while metal nanoparticles in PtRu/C have a good dispersion. This morphological difference is responsible for the observation that the methanol stripping peak of PtRu black is much lower than that of anode with PtRu/C. Although PtRu black and PtRu/C have almost the same alloy degree, PtRu/C shows a higher utilization of Ru and a greater influence of unalloyed Ru on Pt than PtRu black because carbon support could provide electron conduits for more unalloyed Ru that in turn provides more OH species for Pt nanoparticles to oxidize methanol under lower potential. Such catalytic behavior of the unalloyed Ru and the low alloying degree of polyol-synthesized PtRu catalysts make the methanol stripping

peak areas smaller and broader, and peak positions shift to lower anode position than those of the corresponding commercial catalysts.

Acknowledgements

We thank associate Prof. Ying Wan from Shanghai Normal University and associate Prof. Xuming Wei from Dalian Institute of Chemical Physics for the TEM analysis. This work was financially supported by Innovation Foundation of Chinese Academy of Science (K2006D5), Hi-Tech Research and Development Program of China (2006AA05Z137, 2006AA05Z139, 2006AA03Z225), National Natural Science Foundation of China (Grant No.: 50575036 and 50676093), and DUT-DICP Joint Research Foundation.

References

[1] M. Watanebe, S. Motoo, J. Electroananl. Chem. 60 (1975) 267.
[2] J. Munk, P.A. Christensen, A. Hamnet, E. Skou, J. Electroanal. Chem. 401 (1996) 215.
[3] H. Wang, C. Wingender, H. Baltruschat, M. Lopez, M.T. Reetz, J. Electroanal. Chem. 509 (2001) 163.
[4] X. Ren, M.S. Wilson, S. Gottesfeld, J. Electrochem. Soc. 143 (1996) L12.
[5] W. Chen, J. Lee, Z. Liu, Chem. Commun. (2002) 2588.
[6] Z. Liu, X. Ling, X. Su, J. Lee, J. Phys. Chem. B 108 (2004) 8234.
[7] Z. Zhou, S. Wang, W. Zhou, G. Wang, L. Jiang, W. Li, S. Song, J. Liu, G. Sun, Q. Xin, Chem. Commun. (2003) 394.
[8] L. Jiang, G. Sun, S. Sun, J. Liu, S. Tang, H. Li, B. Zhou, Q. Xin, Electrochim. Acta 50 (2005) 5384.
[9] H. Li, Q. Xin, W. Li, Z. Zhou, L. Jiang, S. Yang, G. Sun, Chem. Commun. (2004) 2776.
[10] S. Yan, G. Sun, J. Tian, L. Jiang, Q. Xin, Electrochim. Acta 52 (2006) 1692.
[11] C. Bock, C. Paquet, M. Couillard, G. Botton, B. MacDougall, J. Am. Chem. Soc. 126 (2004) 8028.
[12] Z. Wei, S. Wang, B. Yi, J. Liu, L. Chen, W. Zhou, W. Li, Q. Xin, J. Power Sources 106 (2002) 364.
[13] E. Antolini, F. Cardellini, J. Alloys Compd. 315 (2001) 118.
[14] A.F. Holleman, E. Wiberg, Inorganic Chemistry, Academic Press, 1995.
[15] X. Zhang, K.-Y. Chan, Chem. Mater. 15 (2003) 451.
[16] A.J. Dickinson, L.P.L. Carrette, J.A. Collins, K.A. Friedrich, U. Stimming, J. Appl. Electrochem. 34 (2004) 975.
[17] L. Dubau, C. Hahn, C. Coutanceau, J.M. Leger, C. Lamy, J. Electroanal. Chem. 554–555 (2003) 407.
[18] L. Cao, F. Scheiba, C. Roth, F. Schweiger, C. Cremers, U. Stimming, H. Fuess, L. Chen, W. Zhu, X. Qiu, Angew. Chem. Int. Ed. 45 (2006) 5315.